First evidence for spin-flip $M1$ strength in ^{40}Ar

T. C. Li,[1] N. Pietralla,[1,2] A. P. Tonchev,[3] M. W. Ahmed,[3] T. Ahn,[1,2] C. Angell,[4] M. A. Blackston,[3] A. Costin,[1,2] K. J. Keeter,[5]
J. Li,[6] A. Lisetskiy,[7,*] S. Mikhailov,[6] Y. Parpottas,[3] B. A. Perdue,[3] G. Rainovski,[1] W. Tornow,[3] H. R. Weller,[3] and Y. K. Wu[6]

[1]*Nuclear Structure Laboratory, SUNY at Stony Brook, Stony Brook, New York 11794-3800, USA*
[2]*Institut für Kernphysik, Universität zu Köln, D-50937 Köln, Germany*
[3]*Triangle Universities Nuclear Laboratory, Duke University, Durham, North Carolina 27708, USA*
[4]*Triangle Universities Nuclear Laboratory, University of North Carolina at Chapel Hill, Chapel Hill, North Carolina 27599, USA*
[5]*Department of Physics, Idaho State University, Pocatello, Idaho 83209, USA*
[6]*Duke Free Electron Laser Laboratory, Duke University, Durham, North Carolina 27708, USA*
[7]*National Superconducting Cyclotron Laboratory, Michigan State University, East Lansing, Michigan 48824, USA*

The ^{40}Ar$(\vec{\gamma}, \gamma')$ photon scattering reaction was used to search for spin-flip $M1$ strength in ^{40}Ar. The nearly monochromatic, linearly polarized photon beam of HIγS, in an energy region from 7.7 to 11 MeV, was employed in this study. 28 dipole excitations were observed. The azimuthal intensity asymmetry indicated that all of these states were $E1$ except for the state at $E_x = 9.757$ MeV. Shell-model calculations were used to interpret this state as one fragment of the spin-flip $M1$ strength in ^{40}Ar.

I. INTRODUCTION

Significant progress has recently been made on large-scale shell model calculations for medium-heavy nuclei [1]. In particular, in regions where protons and neutrons occupy the same shell, new interactions have been developed and tested. One example is the GXPF1 interaction proposed by the Tokyo group [2] for the description of nuclei in the $2p1f$-shell. Moreover, single-particle energies are known to evolve with nucleon occupation of orbits [3] and, hence, shell structure evolves with particle number. Lately, interest has been increasing in the challenging cases where protons and neutrons occupy different major shells [4] as, for example, in nuclei where valence protons occupy the sd-shell while valence neutrons occupy the fp-shell. Models for such spaces are important for our understanding of exotic neutron-rich nuclei, including the disappearance and appearance of shell closures through the nuclear chart [5–7].

Additional experimental information on the residual interaction between protons occupying the sd-shell and neutrons occupying the fp shell would improve the predictive power of these model calculations. The ^{40}Ar nucleus has two proton holes in the sd-shell and two neutron particles in the $f_{7/2}$-shell relative to the $N = Z = 20$ shell closure of ^{40}Ca. Information on the level structure and ground state correlations of ^{40}Ar can yield insight into these $2p$-$2h$ interactions.

While collective nuclear properties are well tested by electromagnetic $E2$ transition matrix elements, $M1$ transition matrix elements are more sensitive to single particle aspects of nuclear wave functions. Indeed, strong $M1$ transitions due to proton and neutron spin-flip transitions have been predicted for some time in ^{40}Ar [8]. However, not a single $J^\pi = 1^+$ state of ^{40}Ar has been identified to date [9]. Wickert *et al.* [8] set an upper limit $B(M1) \uparrow < 0.5\mu_N^2$ for individual $M1$ excitations

in ^{40}Ar on the basis of photon scattering data using partially polarized bremsstrahlung, although "strong magnetic spin-flip transitions were expected in ^{40}Ar in the energy region around 9 MeV" [8].

Extensive information on dipole excitations of ^{40}Ar has subsequently been obtained by Moreh *et al.* [10] from photon scattering experiments using unpolarized bremsstrahlung up to 11 MeV. However, these experiments were not sensitive to the parity quantum numbers of the observed dipole excitations.

The availability of quasimonoenergetic, 100% linearly polarized γ-ray beams from the Compton back-scattering of laser light [14–16] has considerably increased the experimental sensitivity for making parity assignments to highly excited dipole states [11–13]. Because of this, we decided to reexamine the long standing puzzle of the predicted yet unobserved magnetic dipole strength around the neutron separation threshold of ^{40}Ar at the HIγS facility.

II. EXPERIMENT

Photon scattering experiments have been performed using the nearly monochromatic, linearly polarized photon beam of HIγS. Eight energy settings with $E_\gamma = 7.8(2)$, 8.2(2), 8.6(3), 8.9(3), 9.5(3), 9.8(3), 10.2(3) and 10.8(3) MeV were used to cover the whole energy range from 7.7 to 11 MeV. Completely polarized γ-ray beams have been generated by laser Compton backscattering of intracavity FEL photons by the relativistic electron beams. The HIγS facility at the Duke FEL is based on the OK-4 storage ring FEL. The OK-4 FEL was tuned to lase at a wavelength of $\lambda = 450$ nm. The electron storage ring was operated at eight energies between 438 and 515 MeV with 14 mA of stored beam current in two bunches.

The Compton backscattered γ-rays were collimated 60 m downstream from the collision point using a Pb collimator having a diameter of 2.54 cm. This geometry results in an energy resolution of approximately 3% for the on-target

---

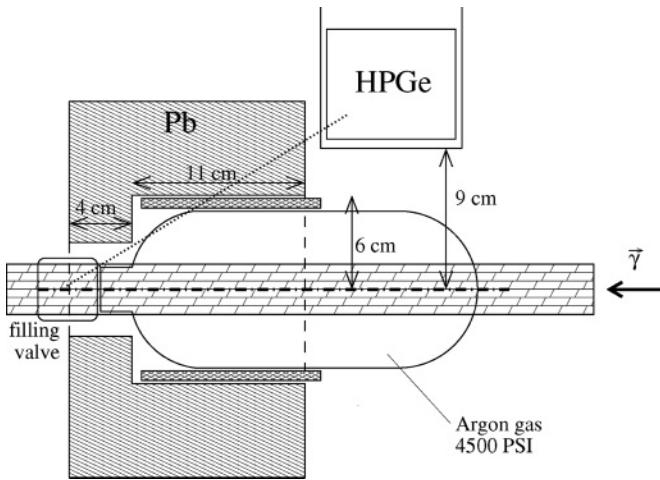*Present address: GSI, D-64291 Darmstadt, Germany.

FIG. 1. Schematic cross section of the arrangement of the argon gas container and the HPGe γ-ray detectors (only one shown, see text).

γ-ray beam. The γ-ray flux on target amounted to about 1.0 photon/(eV s). The target consisted of natural argon gas (99.6% ^{40}Ar) pressurized to 4500 PSI. It was stored in a container consisting of an aluminum core wrapped in carbon fiber, which was placed along the beam axis. Its effective length was 12 cm, giving an effective target thickness of 6.64 g/cm^2. The target holder was a 5-cm-thick Pb ring which also shielded the downstream end of the container, including the filling valve made of brass, from the detectors. Figure 1 shows the cross section of the target setup, argon gas container supported by the target holder, and one of the four HPGe detectors.

The incident beam hit the target to produce scattered photons which were detected by four 60% relative efficiency HPGe detectors mounted at a distance of 9 cm from the beam axis in a polarimeter arrangement. The four detectors were positioned at a mean polar angle of $\bar{\theta} = 90°$ relative to the beam axis and at azimuthal angles of $\phi = 0°, 90°, 180°, 270°$ with respect to the horizontal polarization plane of the incident beam. Two detectors, at azimuthal angles $\phi_\parallel = \{0°, 180°\}$, measured in-plane photon scattering intensity along the polarization direction and the other two, at azimuthal angles $\phi_\perp = \{90°, 270°\}$, measured the out-of-plane intensity perpendicular to it. Data were taken for about 60 h at the above eight energies. The setup was energy calibrated before and after the experimental runs with a ^{11}B target placed at the original target position using an incident beam of $\bar{E}_\gamma = 8.9(3)$ MeV. The excited $\frac{5}{2}^-$ level at 8.92 MeV in ^{11}B and its single escape transition, as well as some background lines, provided good energy calibration points for the high energy range of this experiment, i.e., 7.7 to 11 MeV. For the low energy range, a ^{56}Co source was used for energy calibration up to 3.6 MeV. Relative efficiencies $r(E_\gamma) = \epsilon(\phi_\parallel)/\epsilon(\phi_\perp)$ of the detectors at azimuthal angles $\phi_\parallel, \phi_\perp$ was measured using the data from the ^{11}B and ^{56}Co runs. For example, $r = 0.90(20), 0.76(20)$ at $E_\gamma = 8.5, 9.5$ MeV, respectively. Figure 2 shows nuclear resonance fluorescence (NRF) spectra obtained at azimuthal angles $\phi_\parallel$ and $\phi_\perp$, and mean polar angle $\bar{\theta} = 90°$ from two beam energies $\bar{E}_\gamma = 8.6$ and 9.8 MeV. Peaks labeled with spin and parity quantum numbers represent ground state transitions.

The intensity distribution function derived within the angular correlation formalism [17,18] of a $0^+ \xrightarrow{\vec{\gamma}} 1^\pi \xrightarrow{\gamma} 0^+$
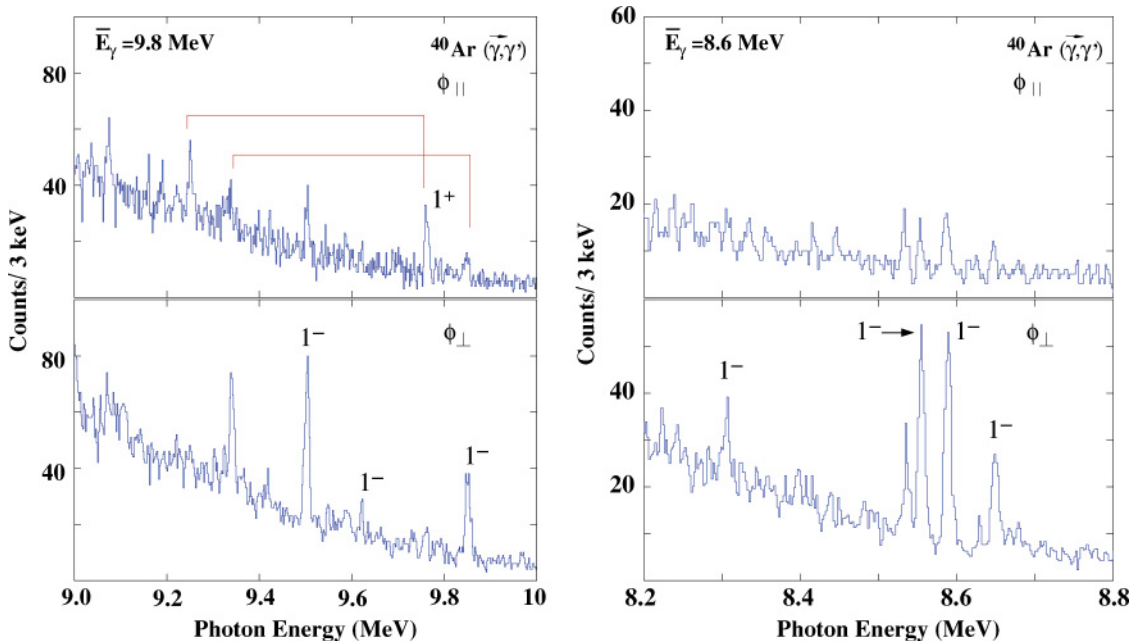

FIG. 2. (Color online) Spectra of the ^{40}Ar$(\vec{\gamma}, \gamma')$ reaction at HIγS. Data were taken at a mean polar angle $\bar{\theta} = 90°$ relative to the incident photon beam and azimuthal angles $\phi_\parallel$ (top) and $\phi_\perp$ (bottom) relative to the polarization plane of the γ-ray beam. The mean γ-ray energy $\bar{E}_\gamma$ of the incident beam is given in the upper left corners. The J^π assignments are indicated for the ground state transitions in ^{40}Ar. The single escape peaks from some ground state transitions are indicated by brackets.

photon scattering cascade is given by [12]

$$W(\theta, \phi) = 1 + \tfrac{1}{2}\left[P_2(\cos\theta) + \tfrac{1}{2}\pi\cos(2\phi)P_2^{(2)}(\cos\theta)\right], \quad (1)$$

with $P_2^{(2)}$ being the unnormalized associated Legendre polynomial of second order and π being the parity quantum number of the dipole excitation. Therefore, the theoretical analyzing power is

$$\Sigma = \frac{W(\phi_\parallel) - W(\phi_\perp)}{W(\phi_\parallel) + W(\phi_\perp)} = \pi = \begin{cases} +1 & J^\pi = 1^+ \\ & \text{for} \\ -1 & J^\pi = 1^- \end{cases}. \quad (2)$$

In the case of an $E2$ excitation for a $0^+ \rightarrow 2^+ \rightarrow 0^+$ cascade, the analyzing power is $\Sigma(E2) = -0.1$.

The experimental asymmetry is

$$A_{\text{expt}} = \frac{A(\phi_\parallel) - r(E_\gamma)A(\phi_\perp)}{A(\phi_\parallel) + r(E_\gamma)A(\phi_\perp)} = Q(E)\Sigma, \quad (3)$$

where $A(\phi)$ represents the peak area in the NRF spectra obtained at $\phi_\parallel$, $\phi_\perp$; and $r(E_\gamma)$ is the measured relative efficiency function. $Q(E)$ is the energy dependent polarization sensitivity of our setup. For this experiment, $Q(E)$ differs from the ideal value $\equiv 1$ due to the spatially extended target and finite solid angles of the detectors. Integrating over the finite range of actual observation angles of the angular distribution functions (1) leads to a partial washing out of the angular correlation effect. Here, $Q(E)$ amounts to about 0.5 independent of energy. Parity quantum numbers of dipole excitations can be assigned from azimuthal intensity asymmetry measured by our detector setup.

III. RESULTS

We observed a total of 28 γ-ray lines. A peak is considered to be a γ-ray line representing a decay transition rather than statistical fluctuation if the measured uncertainty of the peak area extracted from spectra does not exceed 30%. The observed γ-ray transitions can be associated with 28 excited $J = 1$ states of ^{40}Ar between 7.7 and 10.9 MeV. One of them was observed for the first time. It corresponds to a new level in ^{40}Ar and will be discussed in more detail later. Table I summarizes the experimental results. The quoted excitation energies E_x and uncertainties are taken from Ref. [10] unless otherwise noted.

Parity quantum numbers were unambiguously assigned to all the observed levels of ^{40}Ar from the azimuthal intensity asymmetry Σ (see Table I and Fig. 3). 19 of the parity assignments are new while the rest agree with the known parities. Apart from one 1^+ and one $1^{(-)}$ assignment, all other excited states were found to have $J^\pi = 1^-$. The only observed 1^+ state is at 9.757 MeV, contributing a magnetic dipole excitation strength of $B(M1) \uparrow = 0.148(59)\mu_N^2$ in ^{40}Ar. This state will be discussed further. Electromagnetic dipole excitation strengths

$$B(\pi 1) \uparrow = c_{\pi 1} \frac{\Gamma_0}{E_\gamma^3} \quad (4)$$

of the excited states were deduced from information on Γ_0/Γ_γ of Ref. [9], and from Γ_0^2/Γ, Γ_γ/Γ, and Γ of Ref. [10]. Γ_γ, Γ_0, and Γ are total radiative width, ground state decay width, and total width, respectively, of an excited state, and $c_{\pi 1}$
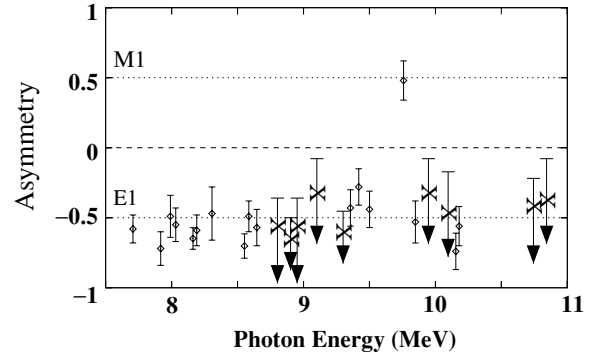

FIG. 3. Asymmetry values A_{expt} of the observed ground state $1^\pi \rightarrow 0_1^+$ transitions for the determination of their radiation character. The polarization sensitivity in this experiment amounted to about 50%. Parity quantum numbers of the corresponding dipole excitations were assigned to be $J^\pi = 1^+$ or 1^- for $M1$ or $E1$ transitions, respectively. Upper limits with centroid values marked as a cross are given for those transitions for which the photon scattering intensity at $\phi_\parallel$ was too weak to be observed. We conclude that only one of the observed excited states has $J^\pi = 1^+$.

is a constant ($c_{E1} = 2.8662 \cdot 10^{-3} \, e^2\text{fm}^2\text{MeV}^3/\text{meV}$, $c_{M1} = 0.2592\mu_N^2 \, \text{MeV}^3/\text{meV}$).

Some aspects of the results require more detailed discussions as given below.

A. Parity assignments

The assignment of parity quantum numbers to the observed $J = 1$ states was solidly based on the photon scattering intensity asymmetry in the azimuthal plane. As displayed in Fig. 3, we could easily distinguish between $M1$ and $E1$ transitions. The possibility of an $E2$ transition is ruled out because all Σ values (or centroid values in the case of upper limits) obtained stay away from $A_{\text{expt}}(E2) = 50\% \times \Sigma(E2) = -0.05$ (see Fig. 3).

30% of the asymmetries are given in upper limits (see Fig. 3). This is because photon scattering intensities at $\phi_\parallel$ for these $E1$ transitions are so weak[1] that only upper limits of peak areas $A(\phi_\parallel)$, typically with large uncertainties, can be extracted. Centroid values for these cases are indicated by a cross in Fig. 3.

For the three transitions ($E_x = 8.834$, 8.883, 8.918 MeV) observed using an incident beam of energy $E_\gamma = 8.9(3)$ MeV, finite values of A_{expt} could not be found because of a gain shift problem in one of the two $\phi_\parallel$ detectors. Nevertheless, we can still unambiguously assign $J^\pi = 1^-$ to all three of them on the basis of the values given in Table I.

B. Level discussion

1. 1^- state at 8.834 MeV.

This state was previously unknown. The $1^- \rightarrow 0_1^+$ transition was not reported from the photon scattering experiment performed by Moreh $et\ al.$ [10] using a bremsstrahlung γ-ray beam probably because the corresponding peak was hidden in

---

[1] For the case of an ideal polarization sensitivity $Q(E) = 1$ one must expect $A(\phi_\parallel) = 0$ for $E1$ excitations.

TABLE I. Parity assignments to the observed dipole excitations from the azimuthal intensity asymmetry A_{expt}. 19 of these parity quantum numbers are assigned for the first time. Electromagnetic excitation strengths $B(\pi 1) \uparrow$ were calculated from information on ground state decay widths Γ_0 from Refs. [9,10]. $B(\pi 1) \uparrow$ cannot be evaluated for those states for which information on Γ_0 is unavailable.

$E_x{}^{\text{a}}$ (± 3 keV)	A_{expt}	J^π ($\hbar$)	$B(E1) \uparrow$ ($10^{-3}\ e^2$ fm^2)	$B(M1) \uparrow$ (μ_N^2)	J^π from Ref. [9]
7708	−0.58(10)	1^-	4.55(69)		1
7917	−0.72(12)	1^-	3.54(46)		1
7993	−0.49(15)	1^-	1.46(26)		1
8032	−0.55(12)	1^-	2.08(37)$^{\text{b}}$		1,2$^+$
8162	−0.648(77)	1^-	10.0(17)$^{\text{b}}$		1^-
8191	−0.59(11)	1^-	3.79(57)		1
8303	−0.47(19)	1^-	1.90(32)		1
8552	−0.702(87)	1^-	2.54(27)		1
8585	−0.49(11)	1^-	3.93(59)		1
8644	−0.57(13)	1^-	1.18(31)		1
8834(4)$^{\text{c}}$	< −0.33	1^-			
8883	< −0.50	1^-	3.36(52)		1
8918	< −0.33	1^-	1.21(53)		1^-
9128	< −0.10	1^-	2.45(49)		1^-
9314(4)$^{\text{c,d}}$	< −0.44	1^-			$(1^-, 2^+)$
9356	−0.43(13)	1^-	2.00(60)		1^-
9416	−0.28(13)	1^-	1.44(72)		1^-
9500	−0.44(13)	1^-	20.1(30)		1^-
9582		$1^{(-)}$	5.0(14)		1^-
9617(3)$^{\text{c,d}}$	< −0.16(26)	1^-			1^-
9757	0.48(14)	1^+		0.148(59)	$1^{(-)}$
9849	−0.53(15)	1^-	29.1(54)$^{\text{b}}$		1^-
9950	< −0.08	1^-	5.1(15)		$1^{(-)}$
10090	< −0.16	1^-	1.31(27)		1
10151	−0.74(13)	1^-	3.07(43)		1
10177	−0.56(14)	1^-	4.09(54)		1
10745	< −0.20	1^-	1.22(24)		1
10857	< −0.06	1^-	1.25(26)		1

$^{\text{a}}$Energy values taken from Ref. [10] except where otherwise noted.
$^{\text{b}}$$B(E1) \uparrow$ values calculated without considering uncertain decay branches.
$^{\text{c}}$Dipole excitations not observed in Ref. [10].
$^{\text{d}}$Energy value taken from Ref. [9].

the triplet formed by escape peaks at nearby energies in their spectra. In our experiment, this transition cannot come from excitation of the material (^{27}Al and ^{12,13}C) of the argon gas container since the closest γ-ray from ^{12,13}C or ^{27}Al is over 25 or 70 keV [19,20,22] away from 8.834 MeV, respectively. In addition, we can rule out the possibility of room background lines being the origin of this new γ ray at 8.834 MeV from their time-correlation with the beam. Moreover, it is impossible that the excitation of the other two Ar isotopes, ^{36,38}Ar, in the target could result in the observed new γ ray because their abundances (0.34% ^{36}Ar, 0.06% ^{38}Ar) were negligible and no γ-rays around this energy have been observed in these isotopes [20,21]. Therefore, the γ-ray line at 8.833 MeV can be interpreted as the ground state decay from a previously unknown level in ^{40}Ar at $E_x = 8.834(4)$ MeV.

2. 1^- state at 9.128 MeV.

This state was known from Ref. [24] as a $J^\pi = 1^-$ state. In the present experiment, it was located at the edge of the

excitation energy region provided by the incident photon beam with $\bar{E}_\gamma = 9.5(3)$ MeV. It was therefore not strongly excited and its ground state transition was observed to be relatively weak. The low statistics caused its $A_{\text{expt}} < -0.10$ (see Table I) to be comparatively high. However, with an A_{expt} centroid value of -0.32 (see Fig. 3) and visible asymmetry observed in the $\phi_\parallel, \phi_\perp$ spectra, we can still assign $J^\pi = 1^-$ to this state, thus confirming the previous assignment.

3. $1^{(-)}$ state at 9.582 MeV.

The ^{36}S$(\alpha, \gamma)^{40}$Ar alpha capture reaction of Cseh *et al.* [24] indicated that this state corresponds to a doublet of levels at 9.580 and 9.585 MeV. They assigned $J^\pi = 1^-, (1^-, 2^+)$ to the levels at 9.580, 9.585 MeV, respectively. In the photon scattering experiment by Moreh *et al.* [10], $J = 1$ was assigned to this doublet state. In the present experiment, the ground state transition of this state was observed to be very weak. This made its value of A_{expt} unreliable and it is therefore not included in

Table I. However, our results do not disagree with previous assignments.

4. 1^- state at 9.617 MeV.

This state was known from Ref. [24] as a $J^\pi = 1^-$ state. Moreh *et al.* [10] did not report observation of its ground state transition probably because its intensity was too weak and/or it was hidden in an escape peak at nearby energy. Although its excitation energy coincides with a level in ^{27}Al, which made up our Argon gas container, at 9.619(3) MeV, no γ ray was observed from that level in previous sensitive photon scattering experiments on ^{27}Al [19,25]. Therefore, the γ-ray line from our data cannot come from ^{27}Al. Our measurement of the corresponding ground state transition was close to the sensitivity limit of our experiment so that our value of A_{expt} is consistent with zero (in Table I, we give the centroid value of its upper limit with the uncertainties). This A_{expt} value is omitted from Fig. 3. However, by observing its intensity asymmetry in the $\phi_\parallel$, $\phi_\perp$ spectra (Fig. 2), we are inclined to assign $J^\pi = 1^-$ to this state, which is in agreement with the literature.

5. 1^- state at 9.950 MeV.

This state was known from Ref. [24] as a $J^\pi = 1^-$ state. Very similar to the state at 9.128 MeV (see above), the excitation energy of this state was located at the edge of the excitation energy region of the $\bar{E}_\gamma = 10.2(3)$ MeV incident beam. Its ground state transition was observed to be weak and corresponds to a relatively high A_{expt} upper limit of -0.08. Nevertheless, the asymmetry observed in the $\phi_\parallel$, $\phi_\perp$ spectra and its A_{expt} centroid of -0.32 (see figure 3) allow us to assign negative parity to this state.

6. 1^- state at 10.857 MeV.

The parity quantum number of this $J = 1$ state [10] was previously unknown. Similar to the state at 9.128 MeV (see above), the ground state transition of this state was observed to be weak, especially in the $\phi_\parallel$ spectrum, and corresponds to a relatively high A_{expt} upper limit of -0.06. Nevertheless, the asymmetry observed in the $\phi_\parallel$, $\phi_\perp$ spectra and its A_{expt} centroid of -0.37 (see Fig. 3) allow us to assign $J^\pi = 1^-$ to this state.

C. Electric dipole strengths

Figure 4 shows the electric dipole excitation strength distribution of the 23 $J^\pi = 1^-$ and one $J^\pi = 1^{(-)}$ states observed in the present experiment. The corresponding $B(E1) \uparrow$ values (see Table I) were calculated whenever information on Γ_0 is available from Refs. [9,10]. The $1^- \rightarrow 2_1^+$ decay transitions of two states at 8.032 and 8.162 MeV, and the $1^- \rightarrow 4_1^+$ decay transition of the state at 9.849 MeV are uncertain [9]. Therefore, we do not take these uncertain decay branches into account in the calculation of their $B(E1) \uparrow$ values. Three states at $E_x = 8.834(1)$, 9.314(4) and 9.617(3) MeV were unknown from Ref. [10] and therefore their $B(E1) \uparrow$ cannot be obtained.
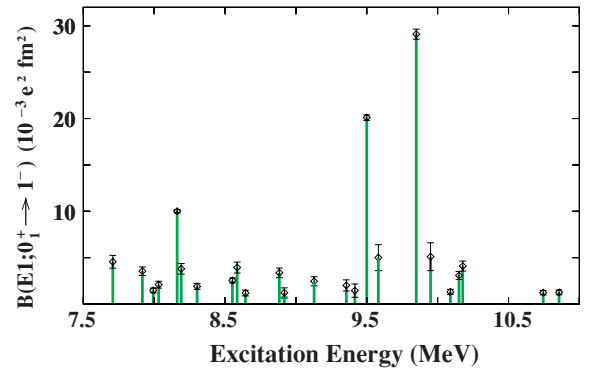

FIG. 4. (Color online) Electric dipole excitation strength $B(E1) \uparrow$ distribution for ^{40}Ar between 7.5 and 11 MeV. The error bars are displayed on top of the data bars (online green).

The two dominant $E1$ excitations at energies of 9.50 and 9.85 MeV carry $E1$ strengths of about 1% of a single particle unit each similar to other findings in this mass region [26]. It can be expected that their wave functions contain considerable components corresponding to $1\hbar\omega$ $1p - 1h$ excitations.

D. Magnetic dipole excitation at $E_x = 9.757$ MeV

The dipole excitation at 9.757 MeV is known [9] from earlier γ-ray spectroscopy following the ^{36}S$(\alpha, \gamma)^{40}$Ar alpha capture reaction studies by Józsa *et al.* [23] and by Cseh *et al.* [24], and from the ^{40}Ar(γ, γ') reaction study of Moreh *et al.* [10]. Moreh *et al.* measured the spin of this state as $J = 1$ but could not determine its parity because an unpolarized photon beam was used. A tentative spin and parity assignment of $(1^-, 2^+)$ was reported by Cseh *et al.* based on the assumption of natural parity.

The spectra in Fig. 2 shows the γ-ray line corresponding to the ground state decay and its single escape transition of the excited state at $E_x = 9.757$ MeV for detectors parallel and perpendicular to the polarization plane of the incident beam. The intensity asymmetry observed clearly proves the $M1$ character of this transition. Therefore, we must assign $J^\pi = 1^+$ to the state at $E_x = 9.757$ MeV in contradiction to the previously made tentative assignment by Cseh *et al.* [24]. This state contributes an $M1$ strength of $B(M1) \uparrow = 0.148(59)\mu_N^2$ in ^{40}Ar. This is the first observation of a 1^+ state in ^{40}Ar.

IV. SHELL MODEL CALCULATION

Shell model calculations were carried out using Nowacki's interaction [27] in which ten valence protons are in the sd-shell and two valence neutrons are in the $f_{7/2} - p_{3/2}$ space in addition to the neutron sd-shell closure, i.e., the 12 neutrons in the sd-shell. Yrast states were well reproduced. Examples are 2_1^+, 4_1^+, and 6_1^+ states calculated at 1.269, 2.820, and 3.569 MeV, respectively. The experimentally measured excitation energies of these states from Ref. [9] are 1.461, 2.893, and 3.464 MeV, respectively. Table II lists the calculated excitation energies E_x, total magnetic excitation strengths $B(M1) \uparrow$ and the strengths due to the proton spin $B(M1_{\sigma_p}) \uparrow$ for the first ten

TABLE II. The excitation energy E_x, total magnetic dipole excitation strength $B(M1) \uparrow$ and strength contributed by the proton spin $B(M1_{\sigma_p}) \uparrow$ for the first ten 1^+ states in ^{40}Ar obtained from shell model calculations as described in the text.

E_x (MeV)	$B(M1) \uparrow$ (μ_N^2)	$B(M1_{\sigma_p}) \uparrow$ (μ_N^2)
4.692	0.428	0.011
5.377	0.031	0.024
6.882	0.197	0.440
8.081	0.005	0.011
8.279	0.015	0.004
9.465	0.107	0.105
9.937	0.005	0.008
10.420	0.036	0.038
11.263	0.007	0.006
12.044	0.004	0.002

1^+ states. For the $M1$ operator we have used a quenching factor of 0.7 for the spin g-factors, 1.1 for the proton orbital g-factor and 0.1 for the neutron orbital g-factor. Figure 5 displays the $M1$ strengths measured in the experiment along with the predictions of this calculation. On the top part, the cross-hatched areas are meant to indicate that the energy regions below 7.7 MeV and above 11 MeV were not investigated in this experiment. A lower limit for the detection of $M1$ strength of 0.05 μ_N^2 was estimated from Ref. [10] for energies between 7.7 and 11 MeV. Any $M1$ strength below this limit could not be detected and therefore this area is also cross-hatched in Fig. 4. The middle and bottom parts of the figure show the distribution of $M1$ strengths and compares the proton spin contribution to the total $B(M1) \uparrow$ for the ten predicted 1^+ states in ^{40}Ar. Among them, the third 1^+ state at 6.882 MeV has the largest proton spin contribution [$B(M1_{\sigma_p}) \uparrow = 0.440 \, \mu_N^2$] to the total $B(M1) \uparrow$. Unfortunately, the mirrors of the optical cavity at HIγS made it impossible at the time of the experiment to cover the energy range below 7.7 MeV and, hence, that dominant fragment of the $\pi(d_{5/2} \rightarrow d_{3/2})$ spin-flip strength could not be investigated. The other state which was dominated by the $\pi(d_{5/2} \rightarrow d_{3/2})$ spin-flip transition is the sixth 1^+ state at 9.465 MeV, which has the second largest proton spin contribution [$B(M1_{\sigma_p}) \uparrow = 0.105 \, \mu_N^2$] to the total $B(M1) \uparrow$. The excitation energies of this predicted 1^+ state at 9.465 MeV and our experimentally identified 1^+ state at 9.757 MeV are very close. The experimental magnetic dipole excitation strength $B(M1_{expt}) \uparrow = 0.148(59) \, \mu_N^2$ agrees with $B(M1_{theo}) \uparrow = 0.107 \, \mu_N^2$ (see Table II) within uncertainties. Based on the excellent agreement of both their E_x and $B(M1) \uparrow$, we interpret the origin of our experimentally identified 1^+ state at 9.757 MeV as one fragment of the proton $d_{5/2} \rightarrow d_{3/2}$ spin-flip transition in ^{40}Ar at that excitation energy. Despite the fact that this is only a small part of the total $d_{5/2} \rightarrow d_{3/2}$ proton spin-flip strength (total $= 2 \, \mu_N^2$, expected), present experimental results supported by the shell model prediction indicate that the proton spin-flip strength is not fully concentrated in the energy interval between 8 and 11 MeV. A similar situation has been observed for ^{36}Ar and ^{38}Ar [21] where the $M1$ strength is even more
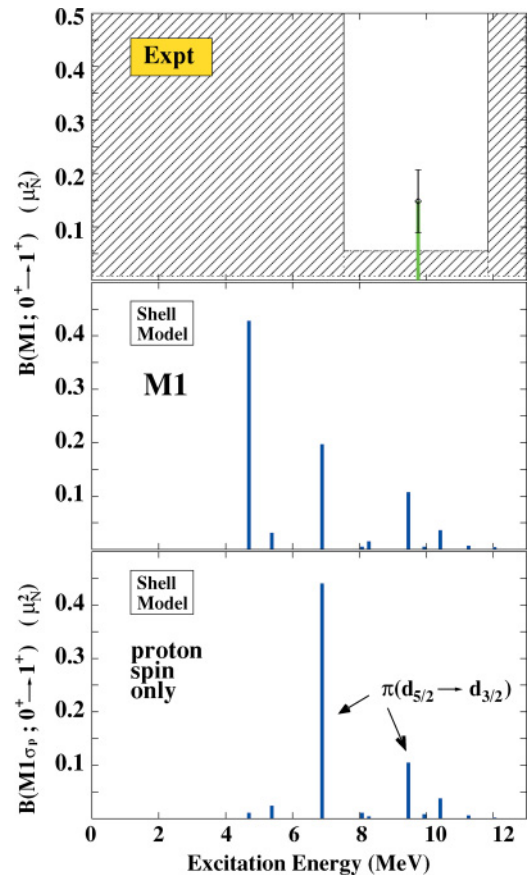

FIG. 5. (Color online) Experimental and theoretical $M1$ strength distributions in ^{40}Ar. (top) The single known 1^+ state observed here at 9.757 MeV within an energy region between 7.7 and 11 MeV. Other energy and strength regions, to which our experiment was insensitive, are shaded. The distribution of the magnetic dipole excitation strengths $B(M1) \uparrow$ (middle) and the proton spin contribution $B(M1_{\sigma_p}) \uparrow$ (bottom) of the first ten 1^+ states predicted by the shell model calculation. Proton $d_{5/2} \rightarrow d_{3/2}$ spin-flip transition strength dominates the $M1$ matrix elements for the third and sixth 1^+ states at 6.882 and 9.465 MeV, respectively, as labeled.

smoothly distributed between 6 and 15 MeV. To gain deeper insight into the structure of argon isotopes near neutron number $N = 20$ and to reveal the role of multiparticle-multihole excitations across the $N = 20$ shell closure it is necessary to investigate experimentally whether the strength in neutron-rich argon isotopes is distributed according to the present shell model picture for ^{40}Ar (Fig. 5, middle and bottom), which shows no cross-shell excitations, or whether it is even more strongly fragmented as in the case of ^{38}Ar.

V. SUMMARY

^{40}Ar($\vec{\gamma}, \gamma'$) photon scattering experiments have been performed using the nearly monochromatic, linearly polarized photon beam of HIγS. Eight beam energy settings have been used to cover the energy range from 7.7 to 11 MeV. 28 dipole excitations within this range were observed and their parity quantum numbers were unambiguously assigned from the azimuthal intensity asymmetry of nuclear resonance

fluorescence. One $M1$ excitation at $E_x = 9.757$ MeV out of all the other $E1$ excitations was identified. Its magnetic dipole excitation strength $B(M1) \uparrow = 0.148(59)\mu_N^2$ was deduced from the literature. Comparison of the data and shell model calculation allows us to interpret this $M1$ excitation as one fragment of the spin-flip $M1$ strength in ^{40}Ar. This is the first evidence for spin-flip $M1$ strength in ^{40}Ar.

[1] E. Caurier, G. Martinez-Pinedo, F. Nowacki, A. Poves, and A. P. Zuker, Rev. Mod. Phys. **77**, 427 (2005), and references therein.

[2] M. Honma, T. Otsuka, B. A. Brown, and T. Mizusaki, Phys. Rev. C **65**, 061301(R) (2002); **69**, 034335 (2004).

[3] T. Otsuka, T. Suzuki, R. Fujimoto, H. Grawe, and Y. Akaishi, Phys. Rev. Lett. **95**, 232502 (2005).

[4] B. A. Brown, Prog. Part. Nucl. Phys. **47**, 517 (2001).

[5] T. Motobayashi *et al.*, Phys. Lett. **B346**, 9 (1995).

[6] V. Tripathi *et al.*, Phys. Rev. Lett. **94**, 162501 (2005).

[7] J. Fridmann, I. Wiedenhöver *et al.*, Nature (London) **435**, 922 (2005).

[8] H. Wickert, K. Ackermann, K. Bangert, U. E. P. Berg, C. Blasing, W. Naatz, A. Ruckelshausen, S. Schennach, and R. Stock, Phys. Rev. C **34**, 835 (1986).

[9] J. A. Cameron and B. Singh, Nucl. Data Sheets **102**, 293 (2004).

[10] R. Moreh, W. C. Sellyey, D. C. Sutton, R. Vodhanel, and J. Bar-Touv, Phys. Rev. C **37**, 2418 (1988).

[11] N. Pietralla, Z. Berant *et al.*, Phys. Rev. Lett. **88**, 12502 (2002).

[12] N. Pietralla *et al.*, Nucl. Instrum. Methods Phys. Res. A **483**, 556 (2002).

[13] A. P. Tonchev *et al.*, Nucl. Instrum. Methods Phys. Res. B **241**, 170 (2005).

[14] V. N. Litvinenko *et al.*, Phys. Rev. Lett. **78**, 4569 (1997).

[15] V. N. Litvinenko *et al.*, Nucl. Instrum. Methods Phys. Res. A **407**, 8 (1998).

[16] S. H. Park *et al.*, Nucl. Instrum. Methods Phys. Res. A **475**, 425 (2001).

[17] L.W. Fagg and S.S. Hanna, Rev. Mod. Phys. **31**, 711 (1959).

[18] N. Pietralla *et al.*, in *Frontiers of Nuclear Structure* [AIP Conf. Proc. No. **656**, 365 (2003)].

[19] P. M. Endt, Nucl. Phys. **A521**, 1 (1990).

[20] P. M. Endt, Nucl. Phys. **A633**, 1 (1998).

[21] C. W. Foltz, D. I. Sober, L. W. Fagg, H. D. Graf, A. Richter, E. Spamer, and B. A. Brown, Phys. Rev. C **49**, 1359 (1994).

[22] F. Ajzenberg-Selove, Nucl. Phys. **A523**, 1 (1991).

[23] M. Józsa, Á. Z. Kiss *et al.*, Nucl. Phys. **A456**, 365 (1986).

[24] J. Cseh and M. Józsa *et al.*, Nucl. Phys. **A489**, 225 (1988).

[25] R. Vodhanel, R. Moreh, W. C. Sellyey, M. K. Brussel, B. H. Wildenthal, Phys. Rev. C **35**, 921 (1987).

[26] T. Hartmann, M. Babilon, S. Kamerdzhiev, E. Litvinova, D. Savran, S. Volz, and A. Zilges, Phys. Rev. Lett. **93**, 192501 (2004).

[27] S. Nummela *et al.*, Phys. Rev. C **63**, 44316 (2001).